Review of Thermal Pulsed Plasma Thruster - Design, Characterization, and Application

IEPC-2015-20／ISTS-2015-b-20
Presented at Joint Conference of 30th International Symposium on Space Technology and Science 34th International Electric Propulsion Conference and 6th Nano-satellite Symposium, Hyogo-Kobe, Japan July 4 – 10, 2015

Yung-An Chan[1], Christoph Montag[2], and Georg Herdrich[3]
University of Stuttgart, Institute of Space Systems (IRS), Stuttgart, Baden-Württemberg, 70569, Germany

and

Tony Schönherr[4]
The University of Tokyo, Department of Aeronautics and Astronautics, Bunkyo, Tokyo, 113-8656, Japan

Abstract: With increasing demand for small satellite, the miniaturization of propulsion system is unavoidable. This forces Pulsed Plasma Thruster (PPT) to operate in a low-energy mode in which their performance is comparatively low. In such case, most of the discharge energy dissipates on Ohmic heating. The performance of low-energy PPT might be dominated by electrothermal acceleration instead of the electromagnetic acceleration. Therefore, the importance of thermal PPT should be re-evaluated. However, no publication yet existed to summarize the development of miniaturized PPT. Therefore, this paper presents the history of the development on low-energy PPT (< 20J), including the design concept and parameter, experiments and numerical model. The important issue in miniaturized PPT will be concerned and discussed.

Nomenclature

B	=	magnetic field
C	=	capacitance
E	=	electric field
e	=	elementary charge
f	=	frequency
g_0	=	gravity constant
I_{sp}	=	specific impulse
I_{bit}	=	impulse bit
$I_{bit_{EM}}$	=	impulse bit contributed by electromagnetic acceleration
$I_{bit_{ET}}$	=	impulse bit contributed by electrothermal acceleration
j	=	current density
k_B	=	Boltzmann constant
L	=	inductance
L_C	=	characteristic length
m_{bit}	=	mass bit

[1] Research associate, Institute of Space Systems, chan@irs.uni-stuttgart.de
[2] Research associate, Institute of Space Systems, montag@irs.uni-stuttgart.de
[3] Head of Plasma Wind Tunnel and Electric Propulsion, Institute of Space Systems, herdrich@irs.uni-stuttgart.de
[4] Assistant Professor, Department of Aeronautics and Astronautics, schoenherr@al.t.u-tokyo.ac.jp

P	=	pressure
P_c	=	critical pressure of PTFE
Q	=	heat flux
R	=	resistance
R_a	=	radius of discharge cavity
Re_{mag}	=	Magnetic Reynold's number
St	=	Stuart number
P	=	pressure
T	=	temperature
T_c	=	critical temperature of PTFE
T_s	=	propellant surface temperature
V_0	=	discharge voltage
V	=	velocity
Γ	=	ablation rate
η_{en}	=	energy transfer efficiency in capacitor
η_{prop}	=	propellant utilization efficiency
η_t	=	thrust efficiency
η_{tran}	=	energy transfer efficiency in electric circuit
κ	=	isentropic index
v_0	=	average exhaust velocity
v_{ei}	=	electron-ion collision frequency
σ	=	plasma conductivity
ϕ	=	plasma potential
AFRL	=	Air Force Research Laboratory
ET	=	electrothermal
EM	=	electromagnetic
IRS	=	Institut für Raumfahrtsysteme
LTE	=	local temperature equilibrium
PPT	=	pulsed plasma thruster
UIUC	=	University of Illinois at Urbana-Champaign

I. Introduction

Since the 1960's, PPTs have been applied for space missions. A PPT offers several advantages that are suitable for satellites, such as simple design, low costs, robustness, low energy consumption, and high reliability.[1] With these advantages, PPTs are attractive candidates for satellite propulsion.

With the general rise of the small satellite market, PPTs are also a target of miniaturization for these last decades.[2] This restriction forces PPTs to operate in a low-power mode in which their performance is comparatively low. In such case, according to the model developed by Laperriere et al.[3], most of the discharge energy is dissipated by Ohmic heating of the propellant. It suggests that the energy applied on electromagnetic acceleration becomes more deficient. In other words, the performance of low-energy PPT might be dominated by electrothermal acceleration instead of the typically expected electromagnetic acceleration. Therefore, the importance of electrothermal PPT (PET) should be re-evaluated, especially in the case of low bank energy.

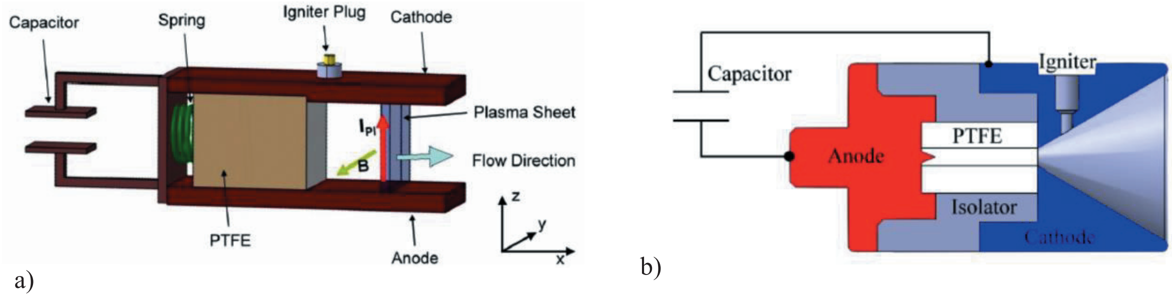

Figure 1. Concept of a) EM-PPT and b) ET-PPT.[4]

The concept and categorization of PPT is well described in several publications. [1,2] The mechanism for thrust generation could be split into two parts: electrothermal (ET) and electromagnetic (EM) acceleration. Fig.1 (a) and (b) are general concepts of PPT with ET and EM acceleration, respectively. For EM-PPT, the thrust is generated by acceleration of the plasma bulk that originates from the current discharge across the propellant surface. The discharge causes ablation and ionization of propellant. The ions are driven by the Lorentz force that is induced by high current density discharge. However, for ET-PPT, as the name tells, the thrust is generated by thermal expansion of propellant which is induced by a gasdynamic effect. Although it loses the property of high exhaust velocity, the ET-PPT in turn has much better thermal efficiency than EM-PPT. In the case of miniaturized PPT, thermal efficiency is an important issue on thruster performance. This implies that ET-PPT might have superiority for miniaturization of PPT. Details are illustrated in Chapter V.

II. Characterization of PPT

PPTs have been characterized for several decades by numerous academic and industrial groups in the world. Generally, the discussion is limited to the improvement of the PPT performance. Before further discussing the parameters of PPTs, a simplification of PPT's operation concept should be introduced at first.

A. Simplified Descriptive Approach for PPT

Fig. 2 shows a simplified PPT concept in the form of an RLC circuit configuration. In addition, this figure generally explains the energy balance in one discharge cycle.

The indices "c", "tran", and "p" represent the capacitor, transmission line, and plasma respectively. The quantity j represents the current flow in the transmission line. E_0, E_t are the stored energy in the capacitor and energy output from thruster. E_{EM} and E_{ET} are the energies provided for ET and EM acceleration respectively.

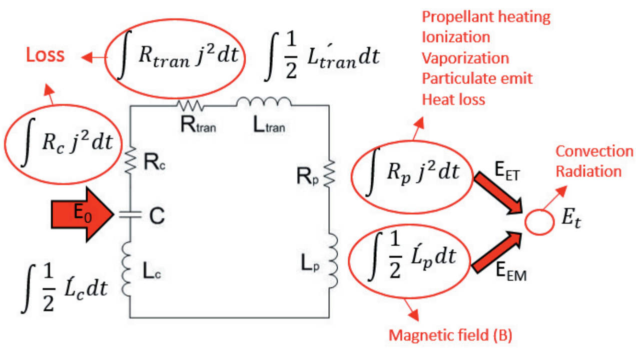

Figure 2. The concept of PPT discharge in RLC circuit.

The energy (E_0) is provided from the external power source to the capacitor. During discharge, energy loss occurs in the capacitor(s) and transition lines. The available energy provided to the thruster is transformed into E_{ET} and E_{EM}, which cause the joule heating on the propellant surface and the formation of magnetic field, respectively. As the plasma bulk is generated and propagated, part of the energy is also dissipated in convection and radiation The rest of energy is transformed into kinetic energy and provides thrust.

B. PPT Performance Evaluation

To evaluate the performance of a PPT, several relevant parameters should be compared and discussed: there are specific impulse (I_{sp}), impulse bit (I_{bit}), thrust efficiency (η_t), and lifetime, respectively. The derivations of these sizes, except for the lifetime, are shown in the following equations:

$$I_{\mathrm{bit}} = I_{\mathrm{bit}_{\mathrm{EM}}} + I_{\mathrm{bit}_{\mathrm{ET}}} = \frac{1}{2}\acute{L} \int j^2\, \mathrm{d}t + m_{\mathrm{bit}}\, v_0 \quad (1)$$

$$I_{\mathrm{sp}} = \frac{I_{\mathrm{bit}}}{m_{\mathrm{bit}}\, g_0\, f} \quad (2)$$

$$\eta_{\mathrm{t}} = \eta_{\mathrm{tran}}\, \eta_{\mathrm{en}}\, \eta_{\mathrm{prop}} \quad (3)$$

where $\acute{L} = \mathrm{d}L/\mathrm{d}x$, v_0 is effective exhaust velocity which includes the contribution of the velocity from ions and neutrals.

The I_{bit} in Eq. (1), as mentioned in chapter I, is contributed by EM and ET acceleration, respectively. With different configurations, the analytical derivation for $\acute{L}$ is different. The equation of $\acute{L}$ is found in the Appendix of Ref. 1. I_{sp} is then calculated after having obtained both the value of I_{bit} and m_{bit} from experiments.

The η_{tran} represents the fraction of the energy transfer from capacitor to discharge. The η_{en} is the efficiency of energy conversion from capacitor to kinetic energy of the plasma bulk. The η_{prop} is defined as the ratio for available accelerated mass bit to total mass bit.[5]

C. List of Parameters

Based on Fig.2 the parameters influencing the thruster performance are listed and discussed generally. From the viewpoint of electric circuit, it is obvious that the resistances (R_p, R_{tran}, R_c) and inductances (L_p, L_{tran}, L_c) of the thruster are strongly connected to the performance. In addition, the energy provided by the capacitor (E_0) is directly related to the available energy for ablation and ionization, both of which are also linked to the thruster performance. Vaporization is controlled by Ohmic heating which is related to the current pass through the surface of propellant (j). It directly determines the plasma generation ($\dot{N}_n + \dot{N}_i + \dot{N}_e$), or said mass bit ($m_{bit}$) and influences the available mass for EM or ET acceleration. The degree of ionization is also related to the discharge current (j) and the propellant surface temperature (T_s). It determines the number of ions ($\dot{N}_i$), in other words, determines the available number of particles that can be driven by Lorentz force.

Form the viewpoint of plasma acceleration, the EM acceleration is determined by the inductance of thruster (L_p) and current density (j). Inductance is determined by the configuration of thruster, electrode materials and conditioning, and propellant. ET acceleration is controlled by the particles density (n_n, n_i, n_e) and translational temperature in plasma bulk (T_n, T_i, T_e) both of which are the parameters for the calculation of kinetic energy. The particle density is connected to the geometry of thruster and the discharge current. The temperature for different particles could be assumed as the same (i.e. $T_n = T_i = T_e$.) due to high particle density during discharge (in the order of 10^{24} m^{-3})[6], which yields LTE.

III. Experiments

To obtain the parameters, such as resistance or inductance, for either deliberating the thruster characteristics or evaluating performance, measurement or modeling methods need to be applied. In this section, the experimental methods for PPT are introduced.

A. Electrical Characteristics

To understand the electrical characteristics, the current waveform is the most critical parameter. It not only could be applied to Eq. (2) to obtain the estimated $I_{bit_{EM}}$, but also could be used for derivation of R_p and L_p by assuming it as an current in underdamped RCL circuit.[7,8] The equations are listed below:

$$j = \frac{V_0}{L\omega C}\, e^{-\frac{R}{2L}t} \sin \omega t \tag{4}$$

$$R = \frac{4L}{T} \ln(\frac{I_1}{I_2}) \tag{5}$$

$$L = \frac{T^2}{4\pi^2 C} \tag{6}$$

where V_0 is voltage, $\omega = (1/LC - R^2/4L^2)$, $T = 2\pi\sqrt{LC}$ is the half period of the waveform.

Two measurement techniques have been applied to obtain the current waveform: Rogowski coil and induction probe. Rogowski coil is a common equipment for measuring high frequency alternative current, and is widely applied in the research of PPT. Induction probes are commonly used for profiling the magnetic field between electrodes[9,10] and the nozzle zone.[11,12,13] Moreover, it could also be used for deriving the current density in space by following Ampère's circuital law ($\boldsymbol{j} = \nabla \times \boldsymbol{B}$). Compared to Rogowski coils, induction probes offer more detailed information of current density distribution in the cavity, which is also an influential issue for thruster performance.

B. Plasma Properties

The discussion of plasma properties in PPT is related to several indexes: particle translational temperature, plasma composition, and plasma velocity. Particle temperature usually resembles as the kinetic energy of particle. Due to assumed LTE in PPT, electron temperature (T_e) is chosen as the index for the calculation of kinetic energy. The second index, plasma composition, could be further divided into the particle density, such as ion, neutral and electron densities (n_n, n_i, n_e), elements (carbon or fluorine in case of PTFE) and charge status (Z_i). Particle densities reflect the degree of ablation and ionization that will eventually influence the amount of impulse contribution by $I_{\mathrm{bit_{ET}}}$ and $I_{\mathrm{bit_{EM}}}$. The elements and charge status will also affect the plasma velocity (U_0^*). But the influences are quite limited.

Several measurement techniques have been applied for investigation of plasma properties for PPT, e.g., electrostatic probe, interferometry, and spectroscopy.

1. Electrostatic Probe

Electrostatic probes are widely used for diagnosis of plasma properties. In PPT research, several kinds of probes were applied including triple electrostatic probes and quadruple electrostatic probes. The triple electrostatic probe had been developed by Habiger[14] to obtain time-dependent information about electron temperature and electron density within the plasma bulk, and it was applied in several research groups.[15] The quadruple electrostatic probe was developed by Burton to measure electron density, electron temperature, and ion Mach number simultaneously.[15] The general theory and comparison of triple probe and quadruple probe can be found in Ref. 17.

2. Interferometry

Interferometry is widely used for measurement of particle density and temperature, or furthermore, plasma velocity. By comparing the phase shift between two light beams (or electromagnetic wave), one of which passes through space for diagnosis and the other passes through empty space as a reference, the properties of plasma can be obtained. The wavelength of the chosen laser beam is determined by the species that one expected to exam. Two kinds of interferometry have been applied on the investigation of PPT: Herriott Cell interferometry[18] and Mach-Zehnder interferometry (MZI)[20,21].

Helmett cell interferometry was developed by Helmett[18] for point measurement by ejecting a laser beam into a Herriott cell that focuses the laser beam on one point as well as increases the path length for the laser beam. This technique was applied at UIUC and AFRL[19].

MZI was applied for investigation for PPT in the University of Tokyo.[20,21] With this technique not only the plasma density and temperature were obtained, but also the plasma front propagation was characterized, which could indirectly allow for the derivation of the plasma velocity.

3. Spectroscopy

Spectroscopy is a useful method to detect the plasma position[15], species of elements, and the charge status. By comparing the intensity of collected light from a high-speed camera, a qualitative analysis of the plasma can be accomplished. Further combining with a database of emission spectroscopy, a quantitative result can be obtained.[22,23] In addition, with high-speed camera, the presence and propagation of different species in different time-steps was acquired,[23] which is important for understanding the detailed phenomena happening inside discharge such as late-time ablation.[24]

C. Other Properties

There are other experimental and diagnostic methods that have been applied for the research of PPT. The general performance indexes, such as thrust, mass bit, and impulse bit, are verified by thrust stand and precision balance. To monitor the propellant surface temperature and energy flux, the thermistor[25, 26] and photovoltaic detector[27] have been applied. To obtain the information about particulate emission, a witness plate was set up to capture the particulates.[28]

IV. Modeling

The numerical model is an important approach for development of PPT. It could offer insightful information for the phenomenon of PPT. Generally, the model for PPT could be separated into three parts: ablation, acceleration, and plume status.

A. Ablation Model

One ablation model was developed by Keidar et al.[29] In that model, it is assumed that a triple-layer structure nearby the surface of heated material exists: a Knudsen layer, a hydrodynamic non-equilibrium layer, and a plasma bulk layer. Fig. 3 shows the schematic of the layer structure near the propellant. The Knudsen layer is a kinetic non-equilibrium layer with a thickness of a few mean free paths of the plasma. The hydrodynamic non-equilibrium layer is a collision-dominated region, but the translational temperature of electrons and heavy particles are different. The outer boundary located between

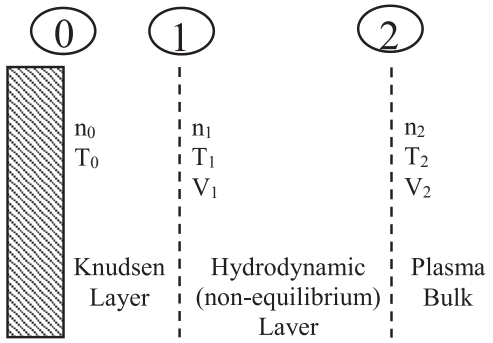

Figure 3. Diagram for the ablation model

hydrodynamic layer and plasma bulk is the surface where all species reach thermal equilibrium.

To understand the ablation rate, the condition of n_0, n_2, T_0, T_2 should be input first. The n_2, T_0, T_2 are obtained by experiments whereas n_0 can be calculated by Eq. (7). By substituting Eq. (8), which is derived by mass and momentum conservation in hydrodynamic layer, to the derivation in Ref. 30, n_1, T_1, and V_1 can be calculated. Then, the ablation rate can be obtained from Eq. (9)

$$P = P_c \exp\left(\frac{T_c}{T_0}\right) = n_0 k_B T_0 \tag{7}$$

$$V_1 = \left[\left(\frac{2kT_1}{m}\right)\left(\frac{T_2 n_2}{2T_1} - n_1/2\right)/\left(n_1 - {n_1}^2/n_2\right)\right]^{0.5} \tag{8}$$

$$\Gamma = mV_1 n_1 = n_1\left[\left(\frac{2kT_1}{m}\right)\left(\frac{T_2 n_2}{2T_1} - n_1/2\right)/\left(n_1 - {n_1}^2/n_2\right)\right]^{0.5} \tag{9}$$

In these equations, P_c and T_c are the critical pressure and temperature of PTFE respectively, m is the molecular weight, and Γ is the ablation rate.

B. Acceleration Model

The acceleration mechanisms in EM-PPT and ET-PPT are quite different. In EM-PPT. the acceleration will focus on the acceleration of charged particles, that is, the interaction of ions and the electromagnetic field caused by the discharge current. The influence of the electromagnetic field is not so important in ET-PPT as the high plasma density inside the whole cavity, which make the LTE and quasi-neutral status established. The magnetic Reynolds number in such high density is far smaller than unity. The effect caused by the magnetic field is then eliminated. The acceleration mechanism will mainly result from the gas-dynamic effect. Eq. (10) to (12) are the equations for the calculation of plasma acceleration: conservation equations of mass, momentum, and energy respectively.

$$A\left(\frac{\partial \rho}{\partial t} + \partial(\rho V)\right) = 2\pi R_a \Gamma(t, z) \tag{10}$$

$$\rho\left(\frac{\partial V}{\partial t} + V\frac{\partial V}{\partial z}\right) = -\frac{\partial P}{\partial z} \tag{11}$$

$$\frac{3}{2} n_e\left(\frac{\partial T}{\partial t} + V\frac{\partial T}{\partial z}\right) = Q_J + Q_r + Q_F \tag{12}$$

In the above equations, R_a is the cavity radius, Q_J is joule heating, Q_r is radiation loss, and Q_F is particle flux respectively. After obtaining the equilibrium pressure and electron temperature, the degree of ionization and plasma composition can be calculated by the Saha ionization equation based on the assumption that the PTFE (C_2F_4) is fully dissociated.

For EM-PPT, the velocity V_2 is increased by the self-induced magnetic field, which might cause the ionization equilibrium unable to be established. Therefore, an assumption of quasi-neutral plasma is not applicable in the case of EM-PPT. To solve the problem, the thermal balance and ablation rate of plasma are treated by Eq. (12) (eliminating the second LHS term) and Eq. (9), respectively. The V_2 will be obtained after solving the condition of plume in section C.

C. Plume

Plume modeling based on a hybrid code of Direct Simulation Monte Carlo (DSMC) method and Particle-In-Cell method (PIC) was applied by Keidar et al.[32, 34] In this model, the quasi-neutrality of plasma in the plume is assumed. Ions and neutrals are treated as particles, whereas electrons are treated as a fluid. Particle collisions are treated by DSMC and the interaction of charged particles with electromagnetic field is treated by PIC. However, the assumption for electron distribution, important for accessing the electric field and magnetic field for PIC, is different for various PPTs. In ET-PPT, the electron distribution is treated as a Boltzmann distribution. The plasma potential can then be calculated by Eq. (13).

$$\phi = T_e \ln\left(\frac{n_e}{n_{ref}(t)}\right) \quad (13)$$

The electric field and magnetic field distributions for EM-PPT are not established under the assumption of a Boltzmann distribution. The electron distribution is derived by electron momentum conservation equation (i.e. Eq. (14)) and Maxwell's equations. Then, the magnetic transport equation becomes Eq. (15)

$$eN_e(\boldsymbol{E} + \boldsymbol{V}_e \times \boldsymbol{B}) = -\nabla \boldsymbol{P}_e - N_e v_{ei} m_e (\boldsymbol{V}_e - \boldsymbol{V}_i) \quad (14)$$

$$\frac{\partial \boldsymbol{B}}{\partial t} = \frac{1}{(\sigma\mu)}\nabla^2 \boldsymbol{B} - \nabla \times \left(\frac{\boldsymbol{j}\times\boldsymbol{B}}{eN_e}\right) + \nabla \times (\boldsymbol{V} \times \boldsymbol{B}) \quad (15)$$

Both the magnetic Reynolds number and the Hall parameter are much lower than unity, thus, the last two RHS terms of Eq. (14) can be eliminated. By introducing Eq. (15) into Maxwell-Faraday's equation and Eq. (14), the electric field and magnetic field are obtained. Then, the ion dynamics can be solved.

V. Optimization Issues of Low-Bank-Energy PPT

A. Miniaturization of PPT

The still growing market of small satellites forces the development of PPTs to miniaturize, both on size and energy level. The low thrust efficiency of PPTs decreases even further.[35] Before considering how to optimize the performance of PPTs, the influence in miniaturization needs to be concerned first.

The most critical issue is the limited power on small satellites. This restricts the available discharge energy for PPTs. Therefore, the consideration of PPTs should focus on the maximum impulse bit per energy (i.e., impulse-to-power ratio).

According to the slug model[7], most of the energy input for a PPT is attributed to Ohmic heating. The rest of energy which could contribute to EM acceleration is only about 10%.[3] In addition, the contribution of $I_{bit_{EM}}$ in impulse bit can be evaluated by the following equation.[4]

$$\frac{I_{bit_{EM}}}{I_{bit}} \le \frac{m_f}{m_{bit}} = \eta_{prop} \quad (16)$$

In the case of Ref. 3, η_{prop} is about 10% and 25% for discharge energies of 1.86 J, and 20 J, respectively. This result infers that the EM acceleration is even smaller in miniaturized PPT. In other words, the ET acceleration needs to be the main consideration for PPT miniaturization.

To prove that statement the following Eq. (17) can be used. Here, the velocity in axial direction (z-direction) of the thruster is described.[36]

$$\frac{\partial v}{\partial z} = \frac{v}{1-M^2}\left\{\frac{\kappa-1}{\rho a^2 v}\frac{j^2}{\sigma} - \frac{1}{\rho a^2}\left(\vec{J}\times\vec{B}\right)_z - \frac{1}{A}\frac{\partial A}{\partial z}\right\} \quad (17)$$

The first summand expresses the influence of ET acceleration, the second summand the influence of the EM acceleration, and the third summand describes the effect of the nozzle. By using Ampère's circuital law with Maxwell's addition, the second term in Eq. (17) can be transformed.

$$\frac{\partial v}{\partial z} = \frac{v_0}{1-M^2}\left\{\frac{\kappa-1}{\rho a^2 v_0}\frac{j^2}{\sigma} + \frac{1}{\rho a^2}\nabla_z\left(\frac{\vec{B}^2}{2\mu_0}\right) - \frac{1}{A}\frac{\partial A}{\partial z}\right\} \quad (18)$$

Furthermore, $\frac{\vec{B}^2}{2\mu_0}$ can be substituted[37]

$$\frac{\vec{B}^2}{2\mu_0} = St\frac{\rho v_0}{L_c\sigma}\frac{1}{2\mu_0} = \frac{St}{Re_{mag}}\frac{1}{2}\rho {v_0}^2 \quad (19)$$

During the process of discharge the magnetic field of the thruster continuously changes which effects the Stuart number and the overall evaluation. To simplify the analysis the magnetic field is assumed to be constant. Therefore, a maximum value of $B = 0.3\ T$ is chosen.[8] This value was found as a maximum for low power thrusters (~20J). Due to the choice of the maximum value the influence of the EM-force will be as large as possible which can be seen as a worst case scenario enrooted within the evaluation. As a result the ratio between St and Re_{mag} can be seen as a length independent factor making it possible to be factorized.

$$\frac{\partial \mathrm{v}}{\partial \mathrm{z}} = \frac{v_0}{1-M^2}\left\{\frac{\kappa-1}{\rho a^2 v_0}\frac{j^2}{\sigma} + \frac{1}{\rho a^2}\frac{St}{Re_{mag}}\nabla_z\left(\frac{1}{2}\rho {v_0}^2\right) - \frac{1}{A}\frac{\partial A}{\partial z}\right\} \tag{20}$$

Since Eq. (17) assumes a flow alone in axial direction, there is only a partial derivative in z-direction necessary, which further can be simplified by using the engineering approach for a 1D-consideration, shown below.

$$\nabla_z = \frac{1}{L_C} \tag{21}$$

The exhaust velocity could be accessed by the definition of thruster efficiency, which is showed in Eq. (22).

$${v_0}^2 = \frac{2\,\eta_T}{m_{bit}}E_0 \tag{22}$$

As it can be seen in Eq. (22) the average exhaust velocity depends on the thruster efficiency and mass bit, both of which could be accessed from experiments. The ratio between η_T and $m_{bit}$is determined analytically based on the data collected in Ref. 38 and the result is shown in Fig. 4.

The tendency of the ratio is illustrated by using a linearly curve fitting and the slope is 1.441. As a result the exhaust velocity in Eq. (22) becomes a linear equation with respect to discharge energy for the overall evaluation. To remind, only data of thrusters where $E_0 \leq 20\ J$are considered within this analysis.

As it can be recognized, three points outline of the curve fitting in Fig.4. These can be explained by the fact that the thruster are the optimized case. Nevertheless, the majority of the data points are still near the approximated curve. Regarding PPTs in the low-energy-region Eq. (21) and Eq. (22), can be inserted into Eq. (20). To remind again, in order to simplify the calculation and accessed the reliable value from experiment, the derivation after Eq. 21 follows on the engineering approach. In Eq. (22), the plasma density ρ could be canceled in the second term on the RHS of equator.

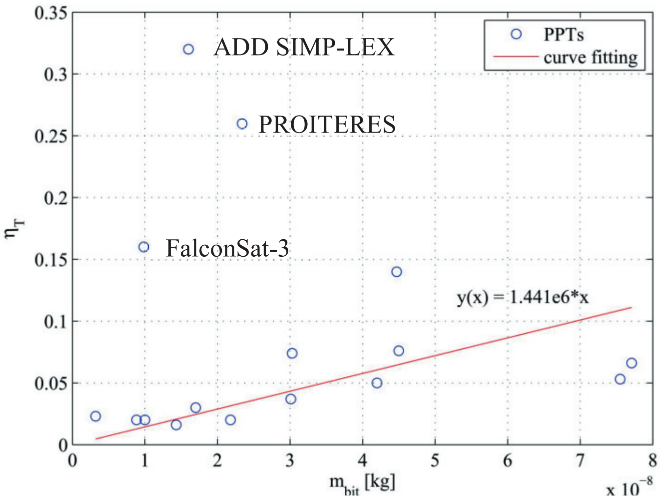

Figure 4. Mass bit and thruster efficiency for PPT with discharge energy below 20 J per pulse.

$$\frac{\partial \mathrm{v}}{\partial \mathrm{z}} = \frac{v}{1-M^2}\left\{\frac{\kappa-1}{\rho a^2\sqrt{1.441\times10^6\,E_0}}\frac{j^2}{\sigma} + \frac{1}{a^2}\frac{St}{Re_{mag}}\frac{1.441\times10^6\,E_0}{L_C} - \frac{1}{A}\frac{\partial A}{\partial z}\right\} \tag{23}$$

Analyzing the Stuart number for energies lower than $20\ J$ results in $St \ll 1$ which means the EM force just has a minor effect to the plasma flow. This implied the dominance of ET acceleration in the case of miniaturized PPTs.

Furthermore, the contribution of EM acceleration is investigated by evaluating the ratio between ET acceleration and EM acceleration with respect to discharge energy. Since the third term on RHS of equator is the thrust contributed by nozzle, it does not have effect in the case of EM-PPT. Therefore, this term can be neglected for the evaluation of EM-PPT. The ratio of the thrust contribution from ET acceleration to EM acceleration is illustrated in Fig. 5.

The analysis has been calculated for three different magnetic fields. Hereby, it allows drawing a conclusion about the tendency of the influence of the EM acceleration compared to ET acceleration for an energy range of $0\,J \leq E_0 \leq 20\,J$. In the calculation, the electron temperature $T_e = 2\,eV$ is assumed[32]. For reasons of simplification, the assumption of constant density ρ is established. In order to evaluate the case with minimum factor of ET acceleration to EM acceleration, a maximum density is chosen base on Ref. 32. The value of conductivity σ could be accesses from, Ref. 37 Moreover, the medium composed by carbon and fluorine is assumed. The velocity is based on calculation of Eq. (22) from the collected data.[38] For the maximum magnetic field of $B = 0.3\,T$ in the case of EM-PPT[8], ET acceleration is at least 15 times larger than the EM acceleration in whole energy band. As the magnetic field decreased, the factor become even larger which indicates the EM acceleration is a minor contributor for the thrust force. As a consequence it is safe to say that the major contribution of thrust for low-energy PPTs is by ET acceleration.

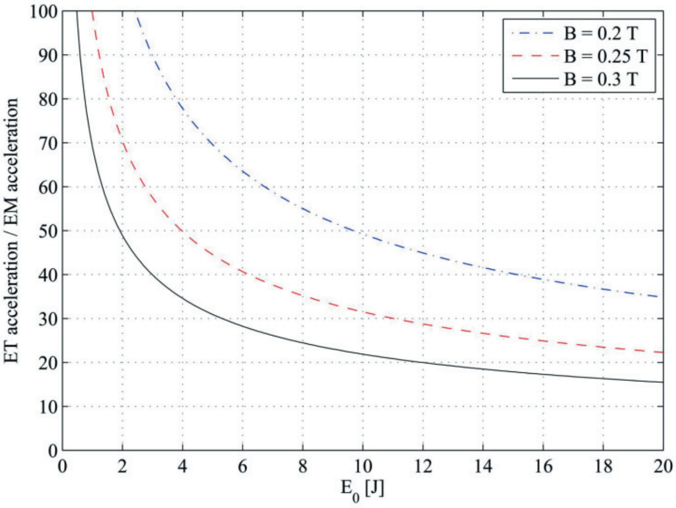

Figure 5. Ratio between the thrust contributed by ET acceleration to EM acceleration along with energy

B. Current Waveform Optimization

From Eq. (1), it is obvious that the current waveform will be one of the main issues for PPT performance. The current waveform can cause inefficient EM acceleration, especially critical for EM-PPT. A non-ideal current waveform is caused by an impedance mismatching between the electric circuit and the thruster. Previous research attempted to regulate the impedance by changing the arrangement of electric circuit, electrode configuration, or the capacitance to obtain an optimum case. Turchi[39] proposed a strategy to improve the performance of thruster by inserting a small impedance across the capacitor rather to damp the current. This would prevent excessive heat generated on the surface of propellant that usually causes the amount of neutrals to increase after the first peak of discharge.[40 41]

Popov and Antropov extended the proposed concept from Turchi to improve the thrust efficiency by changing the discharge current waveform to an aperiodic discharge.[41] For oscillating discharge, the first half-period, which is the most contributive part for EM acceleration, is about 2-3 μs of the entire discharge (about 12-15 μs), whereas the discharge duration for aperiodic mode is about 7-10 μs for APPT in RIAME. The experimental results showed that the thrust efficiency in aperiodic discharge is even twice the case in oscillating discharge. In addition, the measurement of temperature on propellant surface is lower than the prediction by Turchi. The reason of the inefficiency is due to the oscillating discharge which is due to the constriction of distribution current in the volume of dielectric.

Nawaz et al.[42] at IRS derived that the characteristic discharge time $\tau_c = \sqrt{LC}$ influences the thrust efficiency greatly. By changing the capacitance, an optimum thrust efficiency for ADD SIMP-LEX at $\tau_c \cong 2$ μs is obtained, which is the same value predicted by Popov and Antropov in their idea of aperiodic discharge in APPT. The discharge voltage waveform also shows a longer periodic voltage breakdown. It implies that the current waveform in ADD SIMP-LEX is also similar to the aperiodic discharge.

C. Discharge Non-uniformity

The distribution of discharge current is an important issue for PPT. It influences several parameters that are related to the performance of thruster, such as ablation and ionization of propellant, distribution of magnetic field, and lifetime. The non-uniform current flows through a constricted space and returns to electrodes in a specific point. This will form a light spot on either anode or cathode. The probability of this effect increases as the discharge current increases. Keidar et al. started to deliberate the current constriction by developing a model.[6] The optimization of discharge peak current and electrode gap was presented. An explanation was also derived regarding the correlation between the upper limit of mass bit and increased discharge power. That is, when current constriction happened, the current was confined in a small area leading to high local temperatures and high local ablation rates. However, the area for ablation decreases due to the discharge constriction and, therefore, the ablation rate saturates. It suggests that smaller discharge current or electrode gap could help ameliorate the current constriction.

D. Charring Effect

Charring effect is a hazardous problem when considering the thruster lifetime. Several researches show a strong connection of the charring effect with a low energy-to-area ratio.[43,44] The diagnosis of deposition by XEDS showed that the main composition is carbon with slight amount of copper. In addition, the model developed by Keidar el al. also applied to understand the formation of carbon layer.[44] The results show that the region with minimum surface temperature, which is the main factor determined the ablation rate, matches with the position of carbon layer. They concluded that the formation of carbon layer is caused by the returned particles of the plume to the region of lower ablation rate instead of an incomplete decomposition of PTFE.[43] The formation of carbon layer could be restrained by increased energy density on propellant surface which indirectly increasing the ablation rate and reducing the particle back flux.[43]

VI. Conclusion

To follow the small satellite market, the miniaturization of PPT has been continuously progressing for two decades. However, no publication yet existed to summarize the progress, research methods, and issues for this research. Therefore, the conclusions of this study shall be helpful for further development of miniaturized PPT.

A review for miniaturized PPT is presented: concept, experimental methods, modeling approaches, and important issues. In Sec. II, the parameters linked to PPT performance are listed. To obtain these parameters, several experimental (Sec. III) and modeling methods (Sec. IV) are introduced. Finally, the important issues influencing PPT performance are discussed. Suggestions for solving these issues are given along with the discussion. (Sec. V)

First of all, the development strategy for miniaturized PPT shall be focused on the design of electrothermal PPT instead of electromagnetic PPT. According to the evaluation, the thrust contributed by electrothermal acceleration is at least 15 times larger than electromagnetic acceleration in the case with low discharge energy (< 20J). In addition, the design of electric circuit and discharge optimization could almost double the thrust efficiency of PPT. For both cases, ADD SIMPLEX in IRS and APPT in RIAME, the optimization of thrust efficiency was observed when the characteristic time $\tau_c = \sqrt{LC}$ is about 2 μs. Furthermore, the discharge non-uniformity is resulted from XX, which is also the reason why the ablation of propellant does not increase with respect to the discharge energy increase. Lastly, the charring effect has been concluded as a result of the returned particle of the plasma. To diminish the charring effect, the discharge current should be higher than a threshold in order to minimize the returned particles.

Acknowledgments

The first author wants to acknowledge the support of Technologies Incubation Scholarship for PhD study from the Ministry of Education, Taiwan. Further acknowledge go to Professor Keidar for the support on the question in the part of numerical method.

References

[1]Burton, R. L., and Turchi, P. J., "Pulsed Plasma Thruster," *Journal of Propulsion and Power*, Vol.14, No.5, 1998

[2]Molina-Cabrera, P., Herdrich, G., Lau, M., Fausolas, S., Schönherr, T., and Komurasaki, K., "Pulsed Plasma Thruster: A Worldwide Review And Long-Yearned Classification," *32nd International Electric Propulsion Conference,* IEPC-2011-340, Wiesbaden, Germany, 2011

[3]Laperriere, D. D., Gatsonis, N. A., and Demetriou, M. A., "Electromechanical Modeling of Applied Field Micro Pulsed Plasma Thrusters," *41st AIAA/ASME/SAE/ASEE Joint Propulsion Conference & Exhibit*, AIAA-2005-4077, Arizona, USA, 2005

[4]Lau, M. and Herdrich, G., "Pulsed Plasma Thruster Endurance Operation Streaa Tsting at IRS," *33nd International Electric Propulsion Conference,* IEPC-2013-255, Washington, D. C., 2013

[5]Schönherr, T., Komurasaki, K., and Herdrich, G., "Propellant Utilization Efficiency in a Pulsed Plasma Thruster," *Journal of Propulsion and Power*, Vol. 29, No. 6, 2013

[6]Keidar, M., Boyd, I. D., Antonsen, E. L., Burton, R. L., and Spanjers, G. G., "Optimization Issues for a Micropulsed Plasma Thruster," *Journal of Propulsion and Power*, Vol. 22, No. 1, 2006

[7]Jahn, R. G., *Physics of Electric Propulsion*, Dover, New York, 2006, pp. 264, 269, 290.

[8]Pottinger, S. J. and Scharlemann, C. A., "Micro Pulsed Plasma Thruster Development," *30th International Electric Propulsion Conference*, IEPC-2007-125, Florence, Italy, 2007

[8]Spanjers, G. G. and Spores, R. A., "PPT Research at AFRL: Material Probes to measure the Magnetic Field Distribution in a Pulsed plasma thruster- AFRL," *34th AIAA/ASME/SAE/ASEE Joint Propulsion Conference & Exhibit,* AIAA-1998-3659,

Cleveland, OH, USA, 1998

[10]Lau, M. and Herdrich, G., "Plasma diagnostic with inductive probes in the discharge channel of a pulsed plasma thruster," *Vacuum,* 110, 2014, pp. 165-171

[11]Bushman, S. S., Burton, B. L., and Antonsen, E. L., "Arc Measurements and Performance Characteristics of a Coaxial Pulsed Plasma Thruster," *34th AIAA/ASME/SAE/ASEE Joint Propulsion Conference & Exhibit,* AIAA-1998-3660, Cleveland, OH, USA, 1998

[12]Burton, R. L. and Bushman, S. S., "Probe Measurements in a Coaxial Gasdynamic PPT," *35th AIAA/ASME/SAE/ASEE Joint Propulsion Conference & Exhibit,* AIAA-1999-2288, Los Angeles, , CA, USA, 1999

[13]Bushman, S. S. and Burton,R. L., "Heating and Plasma Properties in a Coaxial Gasdynamic Pulsed Plasma Thruster," *Journal of Propulsion and Power*, Vol. 17, No. 5, 2001

[14]Habiger, H. "Elektrostatische Sonden und Fabry-Perot-Interferometrie zur Untersuchung von lichtbogenbeheizten Plasmen für Triebwerksanwendungen und Wiedereintrittssimulation," Dissertation, Institut für Raumfahrtsysteme, Universität Stuttgart, 1994

[15]Nawaz, A., Bauder, U., Böhrk, H. K., and Herdrich, G., "Electrostatic Probe and Camera Measurements for Modeling the iMPD SIMP-LEX," *43rd AIAA/ASME/SAE/ASEE Joint Propulsion Conference & Exhibit*, AIAA-2007-5280, Cincinnati, OH, USA, 2007

[16]Burton, R. L. and Bufton, S. A., "Exit-Plane Electrostatic Probe Measurements of a Low-Power Arcjet," *Journal of Propulsion and Power*, Vol. 12, No. 6, 1996, pp. 1099-1106

[17]Gatsonis, N., Byrne, L., Zwahlen, J., Pencil, E., and Kamhawi, H., "Current-Mode Triple and Quadrupole Langmuir ProbeMethods with Applications to Flowing Pulsed Plasmas," *IEEE Transactions on Plasma Science*, Vol. 32, No. 5, 2004

[18]Herriott, D., Kogelnik, H., and Kompfner, R., "Off-Axis Paths in Spherical Mirror Interferometers," *Applied Optics,* Vol. 3, Issue 4, 1964, pp. 523-526

[19]Antonsen, E. L., Burton, R. L., Spanjers, G. G., and Engelman, S. F., "Herriott Cell augmentation of a quadrature heterodyne interferometer," *Review of Scientific Instrument*, Vol. 74, No. 188, 2003

[20]Shimamura et al., "Internal structure of laser supported detonation waves by two-wavelength Mach-Zehnder Interferometry," *Journal of Applied Physics*, 109, 084910, 2011

[21]Schönherr, T., Nees, F., Arakawa, Y., Komurasaki, K., and Herdrich, G., "Characteristics of plasma properties in an ablative pulsed plasma thruster," *Physics of Plasma*, 20, 033503, 2013

[22]Liu, F., Nie, Z., Xu, X., Zhou, Q., Li, L., and Liang, R., "Measurement of electron density by Stark broadening in an ablative pulsed plasma Thruster," *Applied Physics Letters*, 93, 111502, 2008

[23]Markusic, T. E. and Spores, R. A., "Spectroscopic emission measurements of a pulsed plasma thruster plume," *33rd AIAA/ASME/SAE/ASEE Joint Propulsion Conference*, AIAA-97-2924, Seattle, WA, USA , 1997

[24]Koizumi, H., Noji, R., Arakawa, Y., and Komurasaki, K., "Plasma acceleration processes in an ablative pulsed plasma thruster," *Physics of Plasma*, 14, 033506, 2007

[25]Alexeev, Y. A., Kazeev, M. N., Kozlov, V. F., "Energy Transfer to the Propellant in High Power PPT," Proceedings of the *4th International Spacecraft Propulsion Conference*, ESA SP-555, Sardinia, Italy, 2004

[26]Popov, G. A., Antropov, N. N., Jakovlev, V. N., Tyutin, V. K., Kazeev, M. N., and Kozlov, V. F., "APPT Heat Fluxes Measurement and Calculation," *30th International Electric Propulsion Conference*, IEPC-2007-132, Florence, Italy, 2007

[27]Antonsen, E. L., Burton, R. L., Reed, G. A., and Spanjers, G. G., "Fast Surface temperature measurement of Teflon Propellant-in-pulsed ablative discharge using HgCdTe photovoltaic cells," *Review of Scientific Instrument*, Vol. 77, 103107, 2006

[28]Spanjers, G. G., Lotspeich, J. S., McFall, K. A., and Sproes, R. A., "Propellant Losses Because of Particulate Emission in a Pulsed Plasma Thruster," *Journal of Propulsion and Power*, Vol. 14, No. 4, 1998

[29]Keidar, M., Fan, J., Boyd, I. D., and Beilis, I. I., "On the model of Teflon ablation in an ablation-co trolled discharge," *Journal Physics D: Applied Physics*, 34, 2001, pp. 1675-1677

[30]Keidar, M., Boyd, I. D., and Beilis, I. I., "Vaporization of Heated Materials into Discharge Plasmas," *Journal of Applied Physics*, Vol. 89, No. 6, 3095, 2011

[31]Keidar, M. and Boyd, I. D., "Model of an Electrothermal Pulsed Plasma Thruster," *Journal of Propulsion and Power*, Vol. 19, No. 3, 2003

[32]Keidar, M., Boyd, I. D., Antonsen, E., and Spanjers, G. G., "Electromagnetic Effects in the Near-Field Plume Exhaust of a Micro-Pulsed-Plasma Thruster," *Journal of Propulsion and Power*, Vol. 20, No. 6, 2004

[33]Keidar, M., Boyd, I. D., and Beilis, I. I., "Electric Discharge in the Teflon Cavity of a Coaxial Pulsed Plasma Thruster," *IEEE Transactions on Plasma Science*, Vol. 28, No. 2, 2000 pp. 376-385

[34]Boyd, I. D., Keidar, M., and McKeon, W., "Modeling of a Pulsed Plasma Thruster from Plasma Generation to Plume Far Field," *Journal of Spacecraft and Rocket*, Vol. 37, No. 3, 2000

[35]Gessini et al., "Low Power Ablation Pulsed Plasma Thruster," *33rd International Electric Propulsion Conference*, IEPC-2013-344, Washington, D.C., USA

[36]Auweter-Kurtz, M., and Messerschmid, E.,"*Lichtbogenantriebe für Weltraumaufgaben*," Vieweg+Teubner Verlag, 1992, pp. 54-58

[37]Herdrich, G., "Raumfahrtrelevante Plasmen und deren anwendungsbezogene Klassifizierung," Habilitation Dissertation, Institut für Raumfahrtsysteme, Universität Stuttgart, 2012

[38]Rezaeiha, A. and Schönherr, T., "Review of Worldwode Activities in Liquid-Fed Pulsed Plasma Thruster," *Journal Propulsion and Power*, Vol. 30, No.2, 2014, pp. 253-264

[39]Turchi, P. J., “Directions for Improvement PPT Performance,” *25th International Electric Propulsion Conference*, IEPC-1997-038, Cleveland, Ohio, USA, 2007
[40]Turchi, P. J. and Leiweke, R. J., “Design of an Inductively-Driven Pulsed Plasma Thruster,” *32nd Joint Propulsion Conference and Exhibit*, AIAA-1996-2731, 1996
[41]Popov, G. A., and Antropov, N. N., “Ablative PPT. New quality, new perspectives,” *Acta Astronautica*, 59, 2006, pp. 175-180
[42]Nawaz, A., Albertoni, R., and Auweter-Kurtz, M., “Thrust Efficiency Optimization of the Pulsed Plasma Thruster SIMP-LEX,“ *Acta Astronautica*, 67, 2010, pp. 440-448
[43]Keidar, M., Boyd, I. D., Antonsen, E. L., Gulczinski III, F. S., and Spanjers, G. G., “Propellant Charring in Pulsed Plasma Thruster,” *Journal of Propulsion and Power*, Vol. 20 No. 6, 2004
[44]Mimura, D., Umeda, K., Kitazono, Y., Shindo,, T., Aoyagi, J., and Takegahara, H., “Evaluation of Pulsed Plasma Thruster Performance by Increase of Electric Power,” *32nd International Electric Propulsion Conference*, IEPC-2011-306, Wiesbaden, Germany, 2011